

Viscous corrections for the stability of a two-fluid rotating column

Gennaro Coppola¹, Onofrio Semeraro², Luigi de Luca³

¹*DETEC, Università di Napoli “Federico II”, Italy*

E-mail: gcoppola@unina.it

²*Linné Flow Centre, Department of Mechanics, Royal Institute of Technology, Stockholm, Sweden*

E-mail: onofrio@mech.kth.se

³*DIAS, Università di Napoli “Federico II”, Italy*

E-mail: deluca@unina.it

Keywords: interfacial instability, hydrodynamic stability, rotating flows.

A temporal instability analysis of a two-fluid rotating viscous column enclosed in a rigid cylinder is performed by numerically discretizing the equations for the evolution of disturbances in each phase in the rotating frame of reference. Normal mode analysis applied to such equations leads to two eigenvalue problems, each valid in the region occupied by the single phase fluid and mutually related to each other by the interface conditions. The eigenvalue problem has been solved numerically by suitably discretizing the differential operators by means of a Chebyshev collocation spectral method. A complete investigation of the preferred modes of instability has been carried out over a wide range of the parameter space for the case of the higher density fluid located in the annulus. The behavior of the system in some asymptotic limits of the parameters has been determined and compared to the solutions of simplified corresponding formulations.

1 INTRODUCTION

Viscous rotating immiscible two-fluid systems have attracted the interest of various scientists, since the pioneering studies by Lord Rayleigh [1]. The stability of rotating liquid columns has many applications, ranging from liquid atomization and combustion enhancement to various coating and painting processes.

The basic problem of the stability of a rotating column in absence of gravity and with stress-free boundary conditions has been afforded in the last century by a number of scientists, starting with the work of Hocking and Michael [2] and Hocking [3], who studied the stability of planar disturbances of a uniformly rotating inviscid liquid column. The subsequent works by Gillis [4] and Gillis and Kaufman [5] respectively analyzed the stability of viscous columns with respect to planar and three dimensional disturbances, giving a general stability criterion expressed in terms of the so-called Hocking parameter, measuring the surface tension to centrifugal effects ratio. Only recently, however, a complete investigation of the linear temporal stability of a uniformly rotating viscous liquid column in absence of gravity has been performed by Kubitschek and Weidman [9].

For what it concerns rotating immiscible two-fluid systems, Joseph *et al.* [6] seem to be the first to give a general stability criterion, obtained by minimizing an appropriate potential function. Subsequently, Weidman [8] and Weidman, Goto and Fridberg [11] investigated the linear stability of rigidly rotating immiscible fluids in zero gravity and they were able to obtain a quite complete map of the preferred modes at the onset of instability for the non viscous case as a function of the governing parameters, which are the generalized Hocking parameters for each phase and the density and radius ratios of the two fluid regions. The complete analysis of the viscous case for the two-fluid

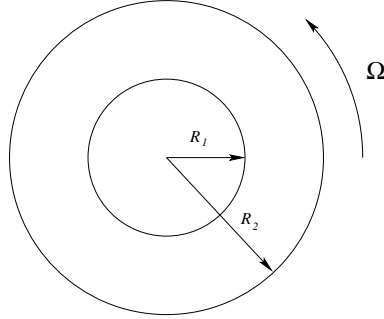


Figure 1: Geometric configuration: inner surface of radius R_1 is the base flow interface, outer surface of radius R_2 is the rigid boundary

rotating column has remained elusive, mainly because of the significant increase in the analytical difficulties and in the number of the governing parameters, which have to include a suitably defined Reynolds number and the viscosity ratio of the two fluids as well. In this paper, a suitable numerical discretization procedure has been employed in order to perform a quite complete analysis of the two-fluid rotating column enclosed in a rigid pipe. By focusing on the case of the heavier fluid in the annulus, the effects of Reynolds number and viscosity and density ratios are analyzed with respect to the non viscous solution.

2 GOVERNING EQUATIONS AND PARAMETERS

2.1 Problem formulation

A pipe of infinite length is filled with two immiscible fluids of constant densities ρ_i and viscosities μ_i , in such a way that the inner cylindrical core fluid of radius R_1 is surrounded by a concentric annulus of the second fluid, which is in turn bounded on the outside by the solid cylinder of radius R_2 (Fig. 1). We adopt the notation that $i = 1$ and 2 refer to core and annular fluids, respectively. The whole system is in uniform rotation around the cylinder axis. We work in cylindrical polar coordinates (r, θ, z) with corresponding unit vectors in the coordinate directions $(\mathbf{e}_r, \mathbf{e}_\theta, \mathbf{e}_z)$. Velocity components are (u_r, u_θ, u_z) and the (constant) angular velocity of rotation is $\Omega = \Omega \mathbf{e}_z$. The unsteady perturbed equations of motions are written in the rotating frame of reference. In each phase they read (here for simplicity the index i is employed for fluid properties only):

$$\begin{aligned} \frac{1}{r} \frac{\partial}{\partial r} (r u_r) + \frac{1}{r} \frac{\partial u_\theta}{\partial \theta} + \frac{\partial u_z}{\partial z} &= 0 \\ \frac{D u_r}{D t} - \frac{u_\theta^2}{r} + \frac{1}{\rho_i} \frac{\partial P}{\partial r} &= 2\Omega u_\theta + \Omega^2 r + \frac{\mu_i}{\rho_i} \left(\nabla^2 u_r - \frac{u_r}{r^2} - \frac{2}{r^2} \frac{\partial u_\theta}{\partial \theta} \right) \\ \frac{D u_\theta}{D t} + \frac{u_r u_\theta}{r} + \frac{1}{r \rho_i} \frac{\partial P}{\partial \theta} &= -2\Omega u_r + \frac{\mu_i}{\rho_i} \left(\nabla^2 u_\theta - \frac{u_\theta}{r^2} + \frac{2}{r^2} \frac{\partial u_r}{\partial \theta} \right) \\ \frac{D u_z}{D t} + \frac{1}{\rho_i} \frac{\partial P}{\partial z} &= \frac{\mu_i}{\rho_i} \nabla^2 u_z \end{aligned}$$

Denoting with $\eta(\theta, z, t)$ the location of the interface, the index $i = 1$ is for $r < \eta$ and the index $i = 2$ is for $r > \eta$. Boundary conditions have to be assigned on the axis and at the external solid boundary. On the cylinder axis ($r = 0$) regularity conditions for u_r, u_θ, u_z and P are required and

will be specified later. At the external boundary velocity has to vanish:

$$u_r = u_\theta = u_z = 0 \quad \text{at} \quad r = R_2.$$

At the interface between the two fluids the continuity of total velocity and of stresses, including surface tension contributions, requires:

$$\begin{aligned} \langle u_r \rangle &= \langle u_\theta \rangle = \langle u_z \rangle = 0 \quad \text{at} \quad r = \eta \\ \langle \boldsymbol{\tau} \rangle \cdot \mathbf{n} &= \gamma \kappa \mathbf{n} \quad \text{at} \quad r = \eta \end{aligned}$$

where \mathbf{n} is the unit normal to the interface, pointing from phase 1 to phase 2, κ the sum of the principal curvatures, γ the surface tension coefficient, and angle brackets denote jump over η (i.e. $\langle a \rangle \equiv a_1 - a_2$). Finally, the kinematic boundary condition at the interface requires:

$$u_r = \frac{\partial \eta}{\partial t} + \frac{u_\theta}{r} \frac{\partial \eta}{\partial \theta} + u_z \frac{\partial \eta}{\partial z} \quad \text{at} \quad r = \eta.$$

By assuming a null velocity base flow perturbed with arbitrary small disturbances the linearized Navier-Stokes equations in the rotating frame of reference are:

$$\begin{aligned} \frac{1}{r} \frac{\partial}{\partial r} (ru) + \frac{1}{r} \frac{\partial v}{\partial \theta} + \frac{\partial w}{\partial z} &= 0 \\ \frac{\partial u}{\partial t} - 2\Omega v + \frac{1}{\rho_i} \frac{\partial p}{\partial r} &= \frac{\mu_i}{\rho_i} \left(\nabla^2 u - \frac{u}{r^2} - \frac{2}{r^2} \frac{\partial v}{\partial \theta} \right) \\ \frac{\partial v}{\partial t} + 2\Omega u + \frac{1}{r\rho_i} \frac{\partial p}{\partial r} &= \frac{\mu_i}{\rho_i} \left(\nabla^2 v - \frac{v}{r^2} + \frac{2}{r^2} \frac{\partial u}{\partial \theta} \right) \\ \frac{\partial w}{\partial t} + \frac{1}{\rho_i} \frac{\partial p}{\partial z} &= \frac{\mu_i}{\rho_i} \nabla^2 w \end{aligned}$$

where (u, v, w) are the components of the velocity perturbation field in cylindrical coordinates and p is the perturbation pressure. The linearized interface position is R_1 . Boundary conditions on the pipe wall are:

$$u = v = w = 0 \quad \text{at} \quad r = R_2$$

while at the interface $r = R_1$ we require:

$$\langle u \rangle = \langle v \rangle = \langle w \rangle = 0 \tag{1}$$

$$u - \frac{\partial \delta}{\partial t} = 0 \tag{2}$$

$$-\langle p \rangle + 2 \left\langle \mu \frac{\partial u}{\partial r} \right\rangle = \left\langle \frac{\partial P}{\partial r} \right\rangle \delta + \gamma \left(\delta_{zz} + \frac{\delta_{\theta\theta}}{R_1^2} + \frac{\delta}{R_1^2} \right) \tag{3}$$

$$\left\langle \mu \left(\frac{\partial u}{\partial z} + \frac{\partial w}{\partial r} \right) \right\rangle = 0 \tag{4}$$

$$\left\langle \mu \left(\frac{\partial v}{\partial r} + \frac{1}{r} \frac{\partial u}{\partial \theta} - \frac{v}{r} \right) \right\rangle = 0 \tag{5}$$

where the linearized expression for the curvature has been employed. $\delta(\theta, z, t)$ denotes the perturbation of the interface radius (i.e. $\eta(\theta, z, t) = R_1 + \delta(\theta, z, t)$) and the base pressure radial gradient jump is given by;

$$\left\langle \frac{\partial P}{\partial r} \right\rangle = \langle \rho \rangle \Omega^2 R_1.$$

2.2 Normal mode analysis

As the flow is periodic in both the azimuthal and axial directions, Fourier decomposition of all flow quantities on these coordinates is assumed. The temporal linear stability problem is studied by applying the normal mode analysis and disturbances are hence taken in the form: $(u, v, w, p, \delta) = (i\tilde{u}, \tilde{v}, \tilde{w}, \tilde{p}, \tilde{\delta})\exp[i(kz + n\theta - \omega t)]$ where $k \in \mathbb{R}$ and $n \in \mathbb{Z}$ are, respectively, the axial and azimuthal wavenumbers and ω is the complex frequency.

Scaling lengths with R_1 , velocities with ΩR_1 , time with Ω^{-1} and pressure with $\rho_2 (\Omega R_1)^2$ one obtains the dimensionless disturbance equations:

$$\omega \tilde{u}_i = 2\tilde{v}_i - \lambda^{i-2} \mathcal{D} \tilde{p}_i + \frac{i}{Re_i} \left[\left(\nabla_{n,k}^2 - \frac{1}{r^2} \right) \tilde{u}_i - \frac{2n}{r} \tilde{v}_i \right] \quad (6)$$

$$\omega \tilde{v}_i = 2\tilde{u}_i + \lambda^{i-2} \frac{n \tilde{p}_i}{r} + \frac{i}{Re_i} \left[\left(\nabla_{n,k}^2 - \frac{1}{r^2} \right) \tilde{v}_i - \frac{2n}{r} \tilde{u}_i \right] \quad (7)$$

$$\omega \tilde{w}_i = \lambda^{i-2} k \tilde{p}_i + \frac{i}{Re_i} \nabla_{n,k}^2 \tilde{w}_i \quad (8)$$

$$0 = \mathcal{D}^* \tilde{u}_i + \frac{n \tilde{v}_i}{r} + k \tilde{w}_i \quad (9)$$

where the same notation has been employed for dimensional and non-dimensional quantities and the two-phase formulation has been explicated by adding a subscript i to velocity and pressure variables.

Non-dimensional interface conditions, enforced on the linearized interface $r = 1$ reads:

$$\langle \tilde{u} \rangle = \langle \tilde{v} \rangle = \langle \tilde{w} \rangle = 0 \quad (10)$$

$$\tilde{u} + \omega \tilde{\delta} = 0 \quad (11)$$

$$-\langle \tilde{p} \rangle + \frac{2i}{Re_2} \langle \chi \mathcal{D} \tilde{u} \rangle = \Psi \tilde{\delta} \quad (12)$$

$$\langle \chi \mathcal{D} \tilde{w} + k \tilde{u} \rangle = 0 \quad (13)$$

$$\langle \chi \mathcal{D}^* \tilde{v} + n \tilde{u} \rangle = 0. \quad (14)$$

In these equations \mathcal{D} stands for derivative with respect to r , \mathcal{D}^* is the polar derivative $\mathcal{D}^* = \mathcal{D} + 1/r$, $\nabla_{n,k}^2$ is the laplacian in cylindrical coordinates acting on a normal mode:

$$\nabla_{n,k}^2 = \frac{1}{r} \frac{\partial}{\partial r} \left(r \frac{\partial}{\partial r} \right) - \frac{n^2}{r^2} - k^2$$

and $\Psi = [\langle \lambda \rangle - L_2 (k^2 + n^2 - 1)]$. The non dimensional quantities χ_i and λ_i are respectively viscosity and density ratios, $\chi_i = \mu_i / \mu_2$, $\lambda_i = \rho_i / \rho_2$, Re_i is the Reynolds number $Re_i = \rho_2 \Omega R_1^2 / \mu_i$ and $L_i = \gamma / \rho_i \Omega^2 R_1^3$ is the generalized Hocking number, measuring the ratio between surface tension and centrifugal forces in each fluid at the interface. Since λ_2 and μ_2 are trivially equal to 1 we will drop the subscript when referring to λ_1 and μ_1 .

At the axis of the pipe, due to singularity of the coordinate system kinematic boundary conditions have to be imposed in order to assure that all physical quantities remain bounded and smooth. Following Ash and Khorrami ([7]) we set, at $r = 0$:

$$\tilde{u}, \tilde{v}, \mathcal{D} \tilde{w} = 0, \tilde{p} \text{ finite} \quad \text{for } n = 0 \quad (15)$$

$$\mathcal{D} \tilde{u}, \tilde{u} + n \tilde{v}, \tilde{w}, \tilde{p} = 0 \quad \text{for } |n| = 1 \quad (16)$$

$$\tilde{u}, \tilde{v}, \tilde{w}, \tilde{p} = 0, \quad \text{for } |n| > 1 \quad (17)$$

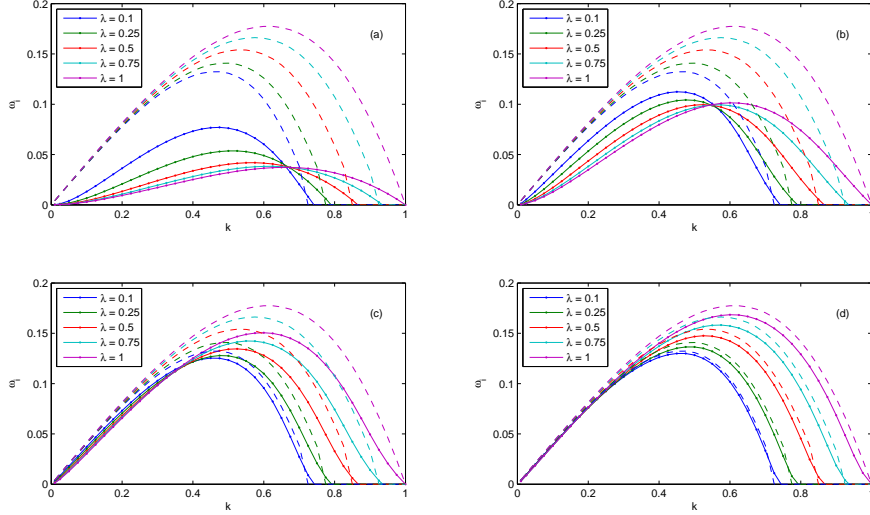


Figure 2: Growth rate vs axial wavenumber. Values of parameters are: $\chi = 1$, $L_2 = 2$, $b = 1.2$. Reynolds number Re_1 is: (a): 10^2 , (b): 10^3 , (c): 10^4 , (d): 10^5

At the external boundary $r = b$, where $b = R_2/R_1$, we have:

$$\tilde{u} = \tilde{v} = \tilde{w} = 0 \quad (18)$$

enforced at $r = b$ where b is the non dimensional external radius: $b = R_2/R_1$. Among the various dimensionless parameters introduced, five of them emerge as independent and we choose to control in our parametric analysis the following: $\lambda, \chi, Re_1, L_2, b$.

3 NUMERICAL TREATMENT

The system of equations (6-9), together with boundary and interface conditions (10-18), can be reduced to a single system of equations for the state vector $\mathbf{q} = (\tilde{u}_1, \tilde{v}_1, \tilde{w}_1, \delta, \tilde{u}_2, \tilde{v}_2, \tilde{w}_2)^T$ by eliminating pressure through equation (8). The corresponding system of equations can be recast in the matrix form:

$$\omega \mathbf{B} \mathbf{q} = \mathbf{A} \mathbf{q}.$$

The system has been discretized by a Chebyshev pseudospectral code written in MATLAB programming language, where each phase has been discretized with a different mesh and interface conditions have been enforced as right and left boundary condition respectively for the inner and outer phase. A simple linear transformation has been employed in order to map each domain to the interval $[-1, 1]$.

We took advantage of the DMSUITE package by Weideman & Reddy [10] in order to generate the required differential Chebyshev operators and boundary and interface conditions are enforced by replacing rows. Kinematic boundary conditions has been imposed as an additional equation associated to the variable δ . By denoting with N_1 and N_2 the number of collocation points for the inner and outer domains, the discretization leads to a generalized matrix eigenvalue problem of

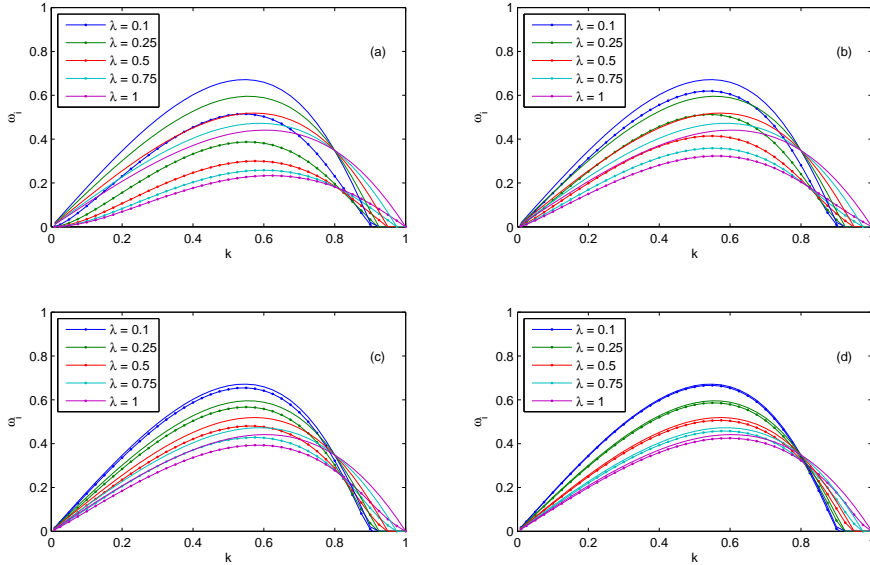


Figure 3: Growth rate *vs* axial wavenumber. Values of parameters are: $\chi = 1$, $L_2 = 5$, $b = 2$. Reynolds number Re_1 is: (a): 10, (b): 10^2 , (c): 10^3 , (d): 10^4

$3N_1 + 3N_2 + 1$ equations, which is solved with the QZ algorithm implemented in the `eig` MATLAB function. Typically, a total number of $N = N_1 + N_2 = 150$ discretization points has been employed.

4 RESULTS

For the problem at hand two limiting situations can be considered, namely the non viscous two-fluid rotating column, and the (viscous) hollow core rotating annulus. The first problem is obtained by formally setting $Re_i = \infty$ and by considering impermeability conditions at pipe wall and continuity of normal velocity and stresses at the interface. This problem has been successfully treated by analytical methods by Weidman, Goto and Fridberg [11], who gave a quite complete treatment of the preferred growth rates for axisymmetric perturbations in terms of Bessel functions. The reproduction of this limiting situation with our code has given excellent results and this has been one of the validation steps of our numerics.

The problem of the viscous hollow core rotating annulus is obtained by setting $\lambda = 0$ and by considering stress-free interface conditions for the annular phase. The results in this limiting case have been obtained with a separate code which discretizes the annular phase and implements the correct interface conditions.

In presenting the results we will mainly focus on two values of the nondimensional external radius $b = 1.2$ and $b = 2$. Since the instability characteristics reach an asymptotic value quite quickly with increasing b , these two values are considered as representative of the narrow and wide gap limits. Moreover, it has been numerically verified that viscosity ratio has a little influence on growth rates, apart from the cases of very low values ($\chi < 0.1$). A representative unit value for

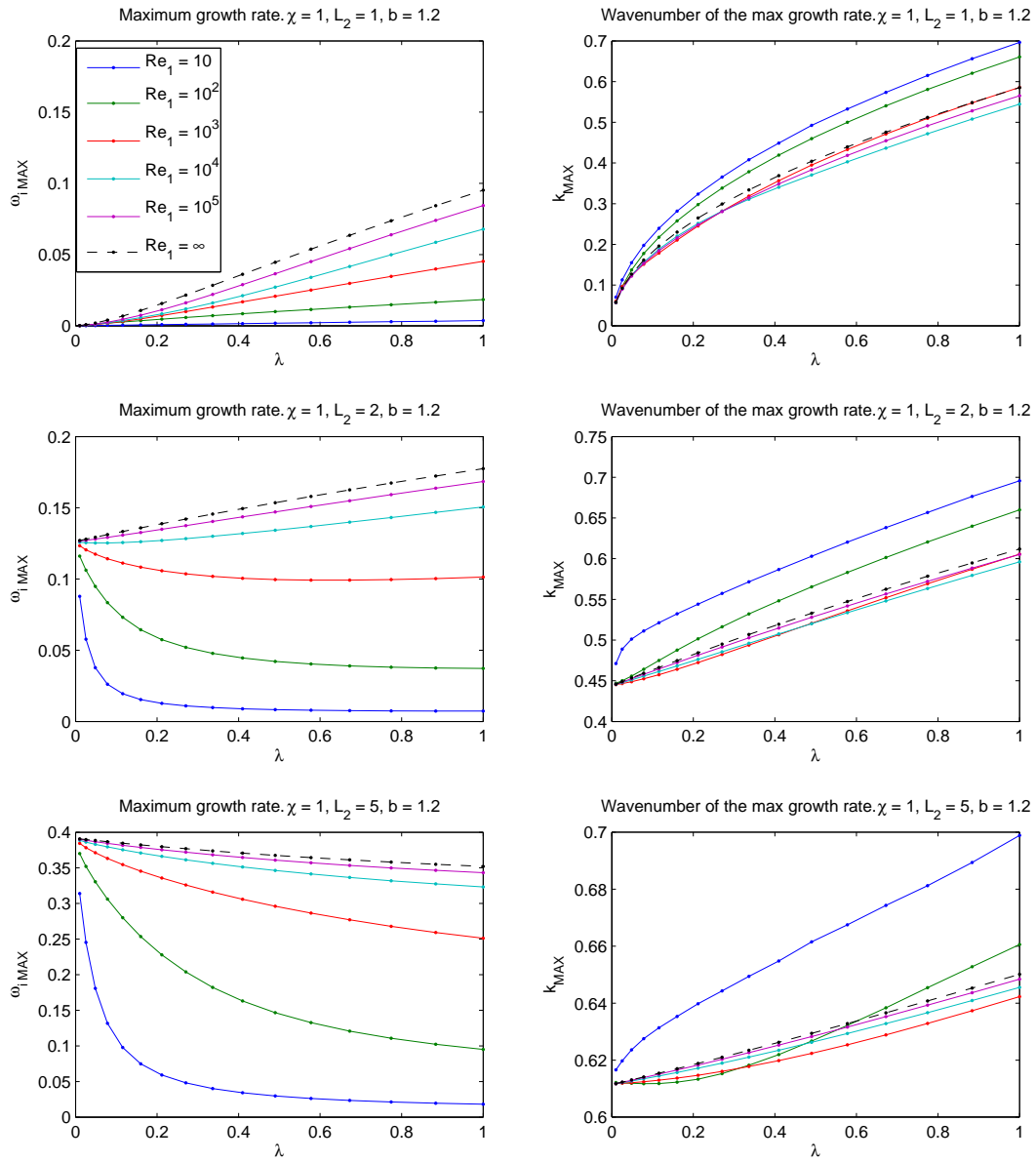


Figure 4: Maximum growth rate and associated wavenumber convergence to inviscid solution vs λ for different Hocking numbers

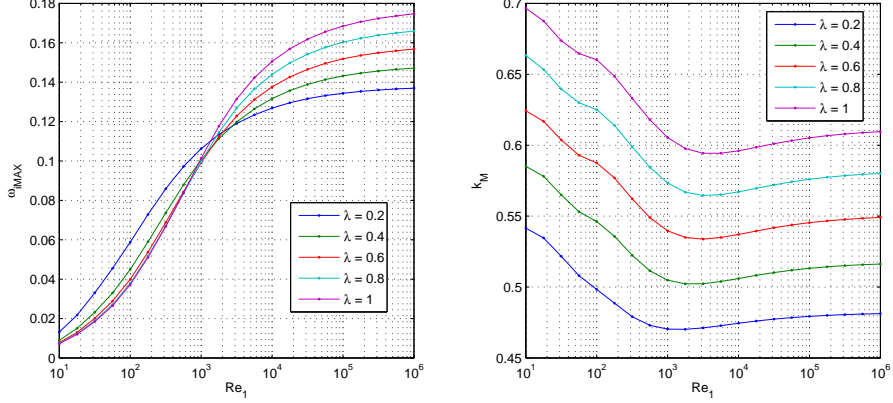


Figure 5: Maximum growth rate (left) and its wavenumber (right) νs Reynolds number at different density ratios. Values of parameters are: $\chi = 1$, $L_2 = 2$, $b = 1.2$.

χ is hence taken for the presentation of the results. Finally, two values $L_2 = 2$ and $L_2 = 5$ for the Hocking number have been considered. They are representative of moderate and high values of surface tension. Note that, as is documented in the studies of the non viscous case (see for example Fig. 12 (a) and 13 (a) of [11]), there is a single value for L_2 at which the maximum growth rate curves exhibit a crossover point with respect to λ . This means that for values of L_2 lower than the crossover value L_{2c} , stability decreases with increasing λ , while for $L_2 > L_{2c}$ increasing λ stabilizes the system. The two values taken for L_2 are representative of the two regimes illustrated.

It is known that in the inviscid limit with $\lambda < 1$ the system loses its stability in correspondence of axisymmetric disturbances. Spotty calculations with our codes of non axisymmetric perturbations have shown no instability still in the corresponding viscous case. The analysis here presented hence focuses on the potentially unstable case of axisymmetric infinitesimal perturbations. We firstly present some representative results in terms of growth rate νs axial wavenumber at different density ratios for various Reynolds numbers.

In Fig. 2 growth rate curves are shown for $L_2 = 2$ and $b = 1.2$ and in the case of equal viscosities. In this and in the following figures dashed lines refer to the non viscous problem. Apart from the obvious role of viscosity in reducing the growth rate, Fig. 2 shows that by taking into account the viscosities of the two fluids some subtle effects arise, affecting the maximum growth rate wavenumber and the role of density ratio in enhancing instability. In fact, while the maximum growth rate is monotonically increasing with density ratio parameter λ in the non viscous case, at low Reynolds numbers this trend is modified in such a way that lower density ratio configurations appear as more unstable. There is a single wavenumber at which the growth rate is independent on the density ratio, and this wavenumber is continuously shifting to shorter wavenumbers as Reynolds number increases. This effect is accompanied by a less visible non monothonical convergence of the maximum instability wavenumber toward its inviscid value.

In Fig. 3 analogous results are presented for the higher surface tension case ($L_2 = 5$) and wide

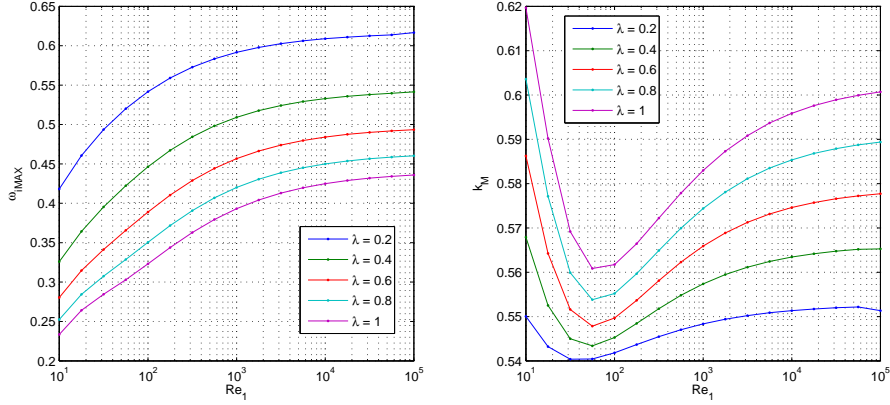


Figure 6: Maximum growth rate (left) and its wavenumber (right) vs Reynolds number at different density ratios. Values of parameters are: $\chi = 1$, $L_2 = 5$, $b = 2$.

gap limit ($b = 2$). It is clearly visible that the crossover point for L_2 has been passed, since the role of λ on the maximum growth rate is reversed with respect to Fig. 2. In this case viscosity does not alter the dependence of maximum growth rate with λ . Note that the high Hocking number case (Fig. 3) reaches its inviscid limit more quickly than the case of Fig. 2. Panels from (a) to (d) in Fig. 3 are relative to Reynolds number values ranging from 10 to 10^4 , while in Fig. 2 we plot the cases from 10^2 to 10^5 .

In order to better visualize the effects mentioned, extensive calculations have been carried out in order to obtain the maximum growth rate with respect to k ; we employed a Golden section search algorithm in order to locate maximum growth rates at different Reynolds numbers and density ratios, usually converging within a few percent of error in 10-15 iterations.

In Fig 4 variations of the maximum growth rate and its axial wavenumber with Reynolds number and density ratios are shown for different values of Hocking number and for $b = 1.2$. The figure clearly shows that the convergence of maximum axial wavenumber to its inviscid value is not monotonic at each fixed value of λ . Moreover, it can be noted how the maximum growth rate curves at low and high values of the Hocking parameter in the non viscous limit are modified by the effects of viscosity.

Fig 5 reports the variation with Reynolds number of the maximum growth rate and of its associated axial wavenumber for the parameters of Fig. 2. The crossover point at which the role of density ratio is reversed is clearly visible in the left plot. This crossover is located at Reynolds number around 10^3 , the inviscid limit being reached at values as high as 10^6 . In the right plot it is showed a non monotonic convergence of the wavenumber of maximum growth rate toward its asymptotic limit. Fig 6, which is relative to the parameters values of Fig. 3, shows that as L_2 exceeds the crossover point L_{2c} , the role of density ratio on the maximum instability growth rate is not affected by viscosity (left panel), while it has still significant effects on the peak wavenumber (right panel).

5 CONCLUSIONS

In this paper, a temporal stability analysis of a two-fluid rotating column, enclosed in a rigid cylinder, has been numerically performed by explicitly taking into account the viscosities of the two fluids. By considering the case of the higher density fluid located in the annulus, a quite complete investigation of the preferred modes of instability has been carried out over representative ranges in the parameter space. It is found that viscosity, in addition to its obvious role of reducing growth rates, plays crucial roles on the selection of the preferred wavenumbers of the fastest growing mode.

References

- [1] Lord Rayleigh “On the instability of cylindrical fluid surfaces,” *Phil. Mag.*, **34**, 177-180 (1892).
- [2] L. M. Hocking and D. H. Michael “The stability of a column of rotating liquid,” *Mathematika*, **6**, 25-32 (1960).
- [3] L. M. Hocking “The stability of a rigidly rotating column of liquid,” *Mathematika*, **7**, 1-9 (1960).
- [4] J. Gillis “Stability of a column of rotating viscous liquid,” *Proc. Camb. Phil. Soc.*, **57**, 152-159 (1961).
- [5] J. Gillis and B. Kaufman “Stability of a rotating viscous jet,” *Q. Appl. Maths*, **19**, 301-308 (1962).
- [6] D. D. Joseph, Y. Renardy, M. Renardy and K. Nguyen “Stability of rigid motions and rollers in bicomponent flows of immiscible liquids,” *Journal of Fluid Mechanics*, **153**, 151-165 (1985).
- [7] R. L. Ash and M. R. Khorrami *Vortex stability* In Fluid Vortices (ed. SI Green), chap. 8, pp. 317-372. Kluwer (1995).
- [8] P. D. Weidman *Stability criteria for two immiscible fluids rigidly rotating in zero gravity*. Revue Roumaine des Sciences Techniques, Serie de Mécanique Appliquée **39**, pp. 481–496 (1994).
- [9] J. P. Kubitschek and P. D. Weidman *The effect of viscosity on the stability of a uniformly rotating liquid column in zero gravity*. Journal of Fluid Mechanics, **572**, pp. 261–286 (2007).
- [10] J. A. C. Weideman and S. C. Reddy *A MATLAB Differentiation Matrix Suite*. ACM Transactions on Mathematical Software, **26**, 4, p. 465, (2000).
- [11] P. D. Weidman, M. Goto and A. Fridberg On the instability of inviscid, rigidly rotating immiscible fluids in zero gravity *Z. angew. Math. Phys.* **48** pp. 921-950, (1997).